Mode identification in the high-amplitude δ Scuti star V2367 Cyg

C. Ulusoy,[1,2]★ T. Gülmez,[1] I. Stateva,[3] D. Dimitrov,[3] I. Kh. Iliev,[3]
H. A. Kobulnicky,[4] B. Yaşarsoy,[5,6] M. Álvarez,[7] R. Michel,[7] L. Fox Machado,[7]
M. Damasso,[8,9] A. Carbognani,[8] D. Cenadelli,[8] T. E. Pickering,[10,11] J. Kwon,[12,13]
M. Tamura[12,13] and L. A. Balona[11]

[1]*Department of Physics, University of Johannesburg, PO Box 524, APK Campus, 2006, Johannesburg, South Africa*
[2]*Department of Physics, Izmir Institute of Technology, 35430, Izmir, Turkey*
[3]*Institute of Astronomy with NAO, Bulgarian Academy of Sciences, blvd.Tsarigradsko chaussee 72, Sofia 1784, Bulgaria*
[4]*Department of Physics and Astronomy, University of Wyoming, PO Box 3905, Laramie, WY 82072, USA*
[5]*Ege University Observatory, 35100, Bornova, Izmir, Turkey*
[6]*Faculty of Arts and Sciences, Astronomy and Space Sciences Department, Inönü University, 44069, Malatya, Turkey*
[7]*Observatorio Astronómico Nacional, Instituto de Astronomía, Universidad Nacional Autónoma de México, Apartado Postal 877,*
22830 Ensenada, BC, Mexico
[8]*Astronomical Observatory of the Autonomous Region of the Aosta Valley (OAVdA), Loc. Lignan 39, I-11020 Nus (Aosta), Italy*
[9]*Department of Physics and Astronomy, vicolo dell'Osservatorio 3, University of Padova, I-35122 Padova, Italy*
[10]*Southern African Large Telescope Foundation, PO Box 9, 7935 Observatory, Cape Town, South Africa*
[11]*South African Astronomical Observatory, PO Box 9, Observatory 7935, Cape Town, South Africa*
[12]*National Astronomical Observatory of Japan, 2-21-1 Osawa, Mitaka, Tokyo 181-8588, Japan*
[13]*Department of Astronomical Science, Graduate University for Advanced Studies (Sokendai), 2-21-1 Osawa, Mitaka, Tokyo 181-8588, Japan*

ABSTRACT

We report on a multisite photometric campaign on the high-amplitude delta Scuti star V2367 Cyg in order to determine the pulsation modes. We also used high-dispersion spectroscopy to estimate the stellar parameters and projected rotational velocity. Time series multicolour photometry was obtained during a 98-d interval from five different sites. These data were used together with model atmospheres and non-adiabatic pulsation models to identify the spherical harmonic degree of the three independent frequencies of highest amplitude as well as the first two harmonics of the dominant mode. This was accomplished by matching the observed relative light amplitudes and phases in different wavebands with those computed by the models. In general, our results support the assumed mode identifications in a previous analysis of *Kepler* data.

Key words: stars: individual: V2367 Cyg – stars: oscillations – stars: variables: δ Scuti.

1 INTRODUCTION

The high-amplitude delta Scuti (HADS) stars are defined as δ Sct stars with peak-to-peak light amplitudes in excess of about 0.3 mag. This amplitude limit is an arbitrary one and there is no other physically identifiable distinction between HADS and other δ Sct stars. The HADS stars rotate more slowly than other δ Sct stars with projected rotationally velocities $v\sin i < 30$ km s^{-1}. They pulsate in one or two dominant modes which are generally assumed to be radial modes, but when observed with greater precision from space many more modes are visible. A large number of combination frequencies and harmonics involving the modes of highest amplitude are

usually present. The pulsational behaviour of HADS stars seems to be intermediate between that of multimode δ Sct stars and Cepheids (Breger 2007). In fact, first-overtone classical Cepheids and HADS stars follow the same period–luminosity relation with no discontinuity (Soszynski et al. 2008).

The reason why δ Sct stars pulsate in many non-radial modes while the more massive Cepheids pulsate only in radial modes is the behaviour of non-radial pulsation modes in the stellar interior. In the deep interior of an evolved giant star such as a HADS star or low-mass Cepheid, non-radial p modes behave like high-order g modes. As the stellar mass increases, these modes develop an increasingly large number of spatial oscillations which leads to increased radiative damping. Therefore we find fewer and fewer non-radial modes in HADS stars of increasing mass until only radial modes are present in what we then call a Cepheid (Dziembowski 1977). Indeed, observations suggest that there is a group of HADS

★ E-mail: cerenuastro@gmail.com

which pulsate just in the fundamental and first-overtone modes with no non-radial modes (Poretti et al. 2005) (they might be called low-mass Cepheids). While this seems to be the main reason why Cepheids do not pulsate in non-radial modes, it may not be the only reason and the problem needs further investigation (Mulet-Marquis et al. 2007).

The study of HADS stars is important because it is an interesting laboratory for investigating mode interaction and non-linear behaviour as exemplified by the presence of combination frequencies. The use of combination frequencies for mode identification is well known in pure g-mode pulsators such as the ZZ Ceti stars (Wu 2001; Montgomery 2005; Yeates et al. 2005). Balona (2012) has recently investigated the problem in pulsating main sequence stars. While in ZZ Ceti stars the combination frequencies arise from interactions in a convective zone in which certain approximations are valid, this is not the case in HADS and it turns out that combination frequencies cannot be used for mode identification.

Mode identification is crucial for extracting stellar parameters from pulsations. The assumption that the modes of highest amplitude in HADS are radial is based on the fact that when two dominant modes are present, their period ratio often agrees with the expected period ratio for first overtone to fundamental radial mode, P_1/P_0, which is in the range 0.77–0.78. The Petersen diagram (Petersen 1973), which is a plot of P_1/P_0 as a function of P_0, is very useful for diagnostic purposes. This ratio varies due to rotation with chemical composition (Poretti et al. 2005) and by coupling with the nearby quadrupole mode (Suárez, Garrido & Goupil 2006; Suárez, Garrido & Moya 2007). The calculated period ratio is also sensitive to the opacity (Lenz et al. 2008).

V2367 Cyg (KIC 9408694) was discovered in a Robotic Optical Transient Search Experiment (ROTSE) survey (Akerlof et al. 2000) and confirmed as a HADS star by Jin et al. (2003) and Pigulski et al. (2009). The star has been observed by the *Kepler* satellite and recently analysed by Balona et al. (2012). The light curve is dominated by a single frequency $f_1 = 5.6611 \, \mathrm{d}^{-1}$ of high amplitude. Two other independent modes with $f_2 = 7.1490 \, \mathrm{d}^{-1}$ and $f_3 = 7.7756 \, \mathrm{d}^{-1}$ have amplitudes an order of magnitude smaller than f_1. Nearly all the light variation is due to these three modes, harmonics of f_1 and combination frequencies with f_1, although several hundred other frequencies of very low amplitude are also present in the *Kepler* photometry.

The star has a much higher projected rotational velocity ($v \sin i = 100 \pm 10 \, \mathrm{km \, s}^{-1}$, Balona et al. 2012) than other HADS stars, which makes it unusual. Such a large rotational velocity complicates the analysis and increases the likelihood of mode interaction. The ratio $f_1/f_2 = 0.792$ is within the expected ratio of second- to first-overtone radial periods which is in the range 0.79–0.80. Balona et al. (2012) attempted to model the observed frequencies as radial modes without mode interaction, but were not successful. A model with mode interaction was found in which f_1 is identified as the fundamental radial mode and f_2 the first-overtone radial mode coupled with a nearby quadrupole mode.

Considering the complex nature of the pulsation, the question arises as to whether the modes f_1 and f_2 are indeed radial and coupled modes as suggested by the models. The model proposed by Balona et al. (2012) would be greatly strengthened if independent mode identification could be made. Since the star is sufficiently bright and of high amplitude, multicolour photometry can be used to provide this verification. The purpose of this paper is to describe a multisite photometric and spectroscopic campaign on V2367 Cyg and subsequent analysis of mode identification.

2 SPECTROSCOPY

The spectra were used to estimate the stellar atmospheric parameters and the projected rotational velocity, $v \sin i$. The spectroscopic observations were carried out with two instruments. The Coudè spectra were obtained with the 2-m RCC telescope of the Bulgarian National Astronomical Observatory, Rozhen. We observed the star during the night of 2011 July 27 in three spectral regions: 4770–4970 Å, 4400–4600 Å and 5090–5290 Å. These three regions contain the Hβ line, Mg II λ4481 Å and a region rich in Fe lines. The instrument uses a Photometrics AT200 camera with a SITe SI003AB 1024 × 1024 CCD (24 μm pixels), giving a typical resolution $R = 16\,000$ and S/N ratio of about 40. The exposure time was 1200 s. The instrumental profile was checked by using the arc spectrum giving a full width at half-maximum (FWHM) of about 0.4 Å. IRAF standard procedures were used for bias subtracting, flat-fielding and wavelength calibration. The final spectra were corrected to the heliocentric wavelengths.

We also obtained spectra with the Wyoming InfraRed Observatory (WIRO) long slit spectrograph which uses an e2V 2048² CCD as the detector. An 1800 lines mm^{-1} grating in first order yielded a spectral resolution of 1.5 Å near 5800 Å with a 1.2 arcsec × 100 arcsec slit. The spectral coverage was 5250–6750 Å. Individual exposure times were 600 s. Reductions followed standard long slit techniques. Multiple exposures were combined yielding final S/N ratios typically in excess of 60 near 5800 Å. Final spectra were Doppler corrected to the heliocentric frame. Each spectrum was then shifted by a small additional amount in velocity so that the Na I D $\lambda\lambda$5890, 5996 lines were registered with the mean Na I line wavelength across the ensemble of observations. This zero-point correction to each observation is needed to account for the effects of image wander in the dispersion direction when the stellar FWHM of the point spread function was appreciably less than the slit width. Because of these inevitable slit-placement effects on the resulting wavelength solutions at the level of ≤10 km s^{-1}, radial velocity standards were not routinely taken.

3 ATMOSPHERIC PARAMETERS

Model atmospheres were calculated using the ATLAS 12 code. The VALD atomic line data base (Kupka et al. 1999), which uses data from Kurucz (1993), was used to create a line list for the synthetic spectrum. Synthetic spectra were generated using the SYNSPEC code (Hubeny, Lanz & Jeffery 1994; Krtička 1998). We adopted a microturbulence of 2 km s^{-1}. The computed spectrum was convolved with the instrumental profile (Gaussian of 0.4 Å FWHM for the Coudè spectra and 1.5 Å FWHM for the WIRO spectra, respectively) and rotationally broadened to fit the observed spectrum under the assumption of uniform rotation.

The best fit to the Hβ and Hα lines was obtained for effective temperature $T_{\mathrm{eff}} = 7250$ K, and surface gravity $\log g = 3.5$. We used the Mg II λ4481 Å line to determine the projected rotational velocity. The best match was obtained with $v \sin i = 90 \, \mathrm{km \, s}^{-1}$. In Fig. 1, we show the best fit to Hβ as well as the fit using two other models with different temperatures for comparison. Our results for the atmospheric parameters and $v \sin i$ are in very good agreement with the results given by Balona et al. (2012) who find $T_{\mathrm{eff}} = 7300 \pm 150$ K, $\log g = 3.5 \pm 0.1$, $v \sin i = 100 \pm 10 \, \mathrm{km \, s}^{-1}$. Uytterhoeven et al. (2011) list the effective temperature as $T_{\mathrm{eff}} = 6810 \pm 130$ K, which is in disagreement with the above values.
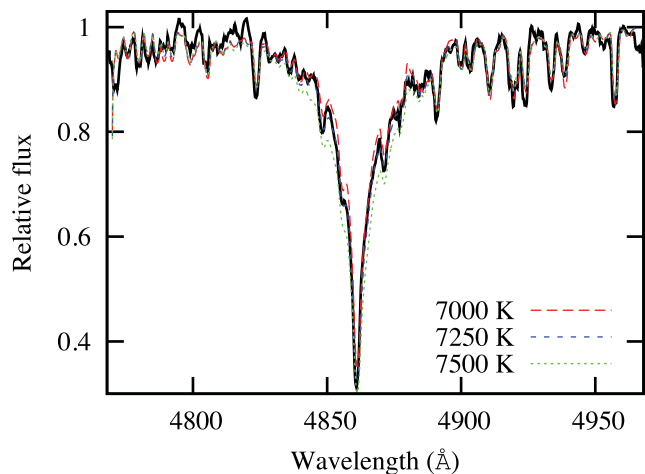
Figure 1. The Hβ line fitted with a model with $T_{\text{eff}} = 7250$ K, $\log g = 3.5$ (cgs) (short dashes). Two other models with $T_{\text{eff}} = 7000$ K (long dashes) and $T_{\text{eff}} = 7500$ K (dots) are given for comparison.

4 PHOTOMETRY

The photometric data were used to determine the amplitude–colour relation and hence the mode for each frequency. The multisite photometric campaign on V2367 Cyg was carried out during 2011 June to 2011 September (Julian dates 245 5726.69–245 5816.52) in Europe and North America with five different sites. Although time allocation for 10 d at KISO Observatory, Japan, was allocated, no photometric data could be obtained due to bad weather. The time of these observations coincides with *Kepler* quarter Q9.3–Q10.3. There are over 127 780 short-cadence (1 min) *Kepler* data points in this time range. Table 1 summarizes the sites, telescopes and additional information regarding the campaign.

Since the aim of this campaign is mode identification, multicolour *UBVRI* filters were chosen. However, Ege University Observatory (EUO) and the Astronomical Observatory of the Autonomous Region of the Aosta Valley (OAVdA) do not have the *U* filter. The *U* filter, when it is used, leads to high signal-to-noise ratio owing to the poor sensitivity of the CCDs in this wavelength and is therefore not reliable. In any case only four nights of *U* photometry are available

Table 1. Information on the photometric multisite campaign. EUO: Ege University Observatory; BNAO-Rozhen: Bulgarian National Astronomical Observatory-Rozhen; OAVdA: The Astronomical Observatory of the Autonomous Region of the Aosta Valley; SPM: Observatorio de San Pedro Mártír; RBO: Red Butte Observatory. Telescope apertures are in m. The total number of nights observed and the start end ending Julian dates of the observations relative to JD 244 550 00 are given.

Observatory	Site	Tel.	CCD
BNAO-Rozhen	Bulgaria	0.60	FLI PL9000
OAVdA	Italy	0.81	FLI PL3041-1-BB
SPM	Mexico	0.84	FLI Fairchild F3041
EUO	Turkey	0.40	Apogee Alta-U47
RBO	USA	0.60	Apogee Alta E47-UV

Observatory	Filters	Dates	Nights
BNAO-Rozhen	*UBVRI*	2	736.34–737.54
OAVdA	*BVRI*	3	737.37–739.56
SPM	*UBVR$_c$I$_c$*	6	718.76–732.98
EUO	*BVRI*	17	736.29–816.52
RBO	*UBVRI*	1	741.68–741.93

which is not sufficient to resolve the frequencies. Although we show the *U* observations in mode identification, they should be given very low weight or ignored. All *R* and *I* filters are of the Johnson/Bessel type except those at Observatorio de San Pedro Mártír (SPM, Mexico) which are of the Cousins/Kron type. The difference is of little consequence as it has a negligible effect on the amplitude ratio and phase difference which are used for mode identification.

When the campaign was initiated in 2011 June, all sites observed the target for three to four nights. Subsequently, only EUO continued to observe the target in July, August and early September. A total of 181 h were spent on observing V2367 Cyg within the 98-d duration of the campaign. Data were reduced using standard IRAF routines including correction for dark, bias and flat-fielding of each CCD frame. The DAOPHOT II package (Stetson 1987) was used for aperture photometry. The observing times were converted to heliocentric Julian Date.

Since *Kepler* photometry was available, it was easy to check the variability of nearby stars. We used the comparison stars GSC 3556 1047 (C1), GSC 3556 1343 (C2) and GSC 3556 627 (C3) because they showed least variability in the *Kepler* photometry (not more than 50 ppm). Because not all instruments have the same field of view, C2 was not observed by some sites and C1 was chosen as the primary comparison star. The data were therefore reduced relative to C1. Outliers produced by poor seeing or transparency variations were removed by visual inspection.

The passbands of corresponding filters in the instruments on different sites are not exactly the same and neither are the optical characteristics of the instruments. Therefore, there are invariably zero-point differences in each filter for each site. Fortunately, we know the frequency composition of the variations in V2367 Cyg from the analysis of the *Kepler* data by Balona et al. (2012). We can assume that the light variations are well modelled by a Fourier series comprising these frequencies where the zero-point will vary from site to site. This is easy to do by fitting the following function to the data by least squares:

$$y_i + \epsilon_i = \sum_{j=1}^{s} \delta_{ij} a_j + \sum_{k=1}^{m} A_k \sin(2\pi f_k t_i + \phi_k), \qquad (1)$$

where y_i is the magnitude at time t_i and ϵ_i is the unknown observational error. The number of different sites is s and $\delta_{ij} = 0$ unless the ith observation is from site j, in which case $\delta_{ij} = 1$. The last term is a truncated Fourier series with m frequencies which represents the variability of V2367 Cyg. By minimizing $\sum \epsilon_i^2$ for $1 \leq i \leq N$ (N being the total number of observations), the individual zero-points for each site, a_j, and the amplitudes and phases of the Fourier series can be found.

In Fig. 2, we show the periodogram of the *V* observations and also of the *Kepler* observations over the same time interval (JD 245 5718.0–245 5817.0). The huge advantage of an uninterrupted time series is very clear in this figure.

We used the first three independent frequencies of highest amplitude obtained by the frequency extraction described in Balona et al. (2012): $f_1 = 5.661\,058$, $f_2 = 7.148\,949$ and $f_3 = 7.775\,566$ d^{-1} together with the first three harmonics of f_1 ($2f_1$, $3f_1$, $4f_1$) for the least-squares Fourier fit (equation 1). Fitting with these six frequencies does not adequately describe the full variation of the star, but is sufficient to determine the zero-points of different sites together with the amplitudes and phases of these particular six frequencies (Table 2). It is these amplitudes and phases which are used in mode identification. From the amplitudes and phases of the fitted-Fourier frequency components, we find amplitude ratios and phase
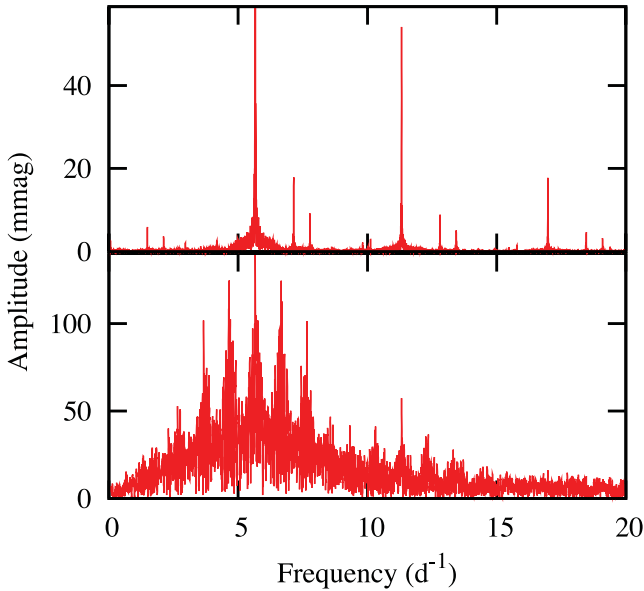
Figure 2. Bottom panel: periodogram of the ground-based *V* observations of V2367 Cyg. Top panel: periodogram of the *Kepler* observations over the same time interval.

differences listed in Table 3 and shown in Fig. 3. Zero points calculated for various sites are shown in Table 4.

The harmonics of the principal frequency, f_1, have large amplitudes and can be used as additional data for mode identification. In fact, the amplitude ratios and phase differences for the harmonics $2f_1$, $3f_1$, are exactly the same as for the fundamental, f_1, as can be seen in Fig. 4. Differential V-band photometry from all sites adjusted for zero-point differences is shown in Fig. 5. Also shown is the fitted-Fourier curve using the six frequencies.

5 MODE IDENTIFICATION

There are several techniques that can be used to discriminate between different values of the spherical harmonic degree, l. In the simplest technique, the amplitude ratios relative to a given waveband are compared with the calculated amplitudes ratios. The method relies on the fact that the variation of light amplitude in different wavelength bands depends on l and is independent of the azimuthal number m. It should be noted that our current models for photometric mode identification are only valid in the limit of no rotation. The rotation introduces departures from pure spherical harmonics so that a single value of l is not sufficient to describe the eigenfunction perfectly. However, so long as the rotation is not very rapid, a single value of l is still a reasonable approximation. We expect that for V2367 Cyg this will be the case, but the relative amplitudes will be modified to some degree due to this effect.

The most general expression for the magnitude variation, m_λ, at wavelength λ for a star pulsating with spherical harmonic degree, l, and angular frequency of pulsation, ω, with angle of inclination, i, is

$$\Delta m_\lambda = -\frac{2.5}{\ln 10}\epsilon P_l^m(\cos i)b_{l\lambda}\{(1-l)(l+2)\cos(\omega t)$$
$$+f_T(\alpha_{T\lambda}+\beta_{T\lambda})\cos(\omega t+\psi_T)-f_g(\alpha_{g\lambda}+\beta_{g\lambda})\},$$

where ϵ is the amplitude of the radial displacement, P_l^m is the associated Legendre polynomial, $f_T = \delta T_{\rm eff}/T_{\rm eff}$ is the amplitude of local effective temperature variation, $f_g = \delta g_e/g_e$ is the am-

Table 2. Amplitudes, *A* (mmag), and phases ϕ (radians) for the three frequencies of highest amplitude: $f_1 = 5.661\,06$, $f_2 = 7.148\,95$, $f_3 = 7.775\,57$ d^{-1} and harmonics of f_1. The epoch of phase zero is JD 245 5700.000.

Frequency	A	ϕ
		U
f_1	248.9 ± 1.5	2.3343 ± 0.0060
$2f_1$	77.5 ± 1.4	2.5586 ± 0.0177
f_2	24.0 ± 1.4	-0.5104 ± 0.0586
$3f_1$	24.7 ± 1.4	2.7732 ± 0.0551
f_3	11.9 ± 1.5	-0.7500 ± 0.1249
$4f_1$	12.5 ± 1.4	2.6230 ± 0.1090
		B
f_1	243.4 ± 1.1	2.2941 ± 0.0043
$2f_1$	75.2 ± 1.0	2.4873 ± 0.0140
f_2	26.5 ± 1.1	-0.5388 ± 0.0403
$3f_1$	22.4 ± 1.0	2.7301 ± 0.0467
f_3	15.1 ± 1.1	-0.7942 ± 0.0706
$4f_1$	11.4 ± 1.0	2.7762 ± 0.0918
		V
f_1	186.9 ± 0.7	2.2641 ± 0.0035
$2f_1$	55.1 ± 0.6	2.4618 ± 0.0117
f_2	19.4 ± 0.7	-0.4727 ± 0.0351
$3f_1$	16.0 ± 0.6	2.7474 ± 0.0401
f_3	10.8 ± 0.7	-0.7081 ± 0.0623
$4f_1$	7.9 ± 0.6	2.7543 ± 0.0806
		R
f_1	141.7 ± 0.7	2.2406 ± 0.0050
$2f_1$	44.9 ± 0.7	2.4660 ± 0.0155
f_2	17.3 ± 0.7	-0.3476 ± 0.0407
$3f_1$	13.6 ± 0.7	2.8603 ± 0.0516
f_3	9.5 ± 0.7	-0.5988 ± 0.0746
$4f_1$	6.2 ± 0.7	2.6144 ± 0.1124
		I
f_1	113.0 ± 0.6	2.1942 ± 0.0055
$2f_1$	36.2 ± 0.6	2.4433 ± 0.0169
f_2	13.7 ± 0.6	-0.4963 ± 0.0449
$3f_1$	10.6 ± 0.6	2.8294 ± 0.0579
f_3	8.3 ± 0.6	-0.6936 ± 0.0746
$4f_1$	5.3 ± 0.6	2.6109 ± 0.1147

plitude of the local gravity variation for unit radial displacement at the photosphere and ψ_T is the phase difference between effective temperature variation and radial displacement. The quantity $b_{l\lambda} = \int_0^1 \mu h_\lambda P_l(\mu)\mathrm{d}\mu$ where the normalized limb darkening function is given by h_λ and $\mu = \cos\theta$ is the polar angle in the spherical coordinate system where the *z*-axis is the line of sight to the observer.

The first term within the bracket in the above expression represents the change in magnitude caused by the geometrical variation of the star during pulsation and is independent of wavelength. The other two terms are wavelength dependent and lead to a variation of amplitude and phase with waveband. The differences in amplitude and phase at different wavebands are small and accurate multicolour photometry is required for good discrimination in l. Mode discrimination is improved by using wavebands covering as wide a wavelength range as possible.

The quantities $\alpha_{T\lambda}$, $\beta_{T\lambda}$, $\alpha_{g\lambda}$, $\beta_{g\lambda}$ are defined in Balona & Evers (1999) and can be determined from static model atmospheres. The assumption that at any instant the atmosphere of a pulsating star

Table 3. Amplitude ratios, A/A_B, and phase differences $\phi - \phi_B$ (radians) relative to the B band for six frequencies of highest amplitude: $f_1 = 5.661\,06, f_2 = 7.148\,95, f_3 = 7.775\,57\,\mathrm{d}^{-1}$.

Filters	A/A_B	$\phi - \phi_B$
	f_1	
U	1.0226 ± 0.0077	0.0402 ± 0.0074
B	1.0000 ± 0.0064	0.0000 ± 0.0061
V	0.7679 ± 0.0045	-0.0300 ± 0.0055
R	0.5822 ± 0.0039	-0.0535 ± 0.0066
I	0.4643 ± 0.0032	-0.0999 ± 0.0070
	$2f_1$	
U	1.0306 ± 0.0231	0.0713 ± 0.0226
B	1.0000 ± 0.0188	0.0000 ± 0.0198
V	0.7327 ± 0.0126	-0.0255 ± 0.0182
R	0.5971 ± 0.0122	-0.0213 ± 0.0209
I	0.4814 ± 0.0102	-0.0440 ± 0.0219
	f_2	
U	0.9057 ± 0.0648	0.0284 ± 0.0711
B	1.0000 ± 0.0587	0.0000 ± 0.0570
V	0.7321 ± 0.0403	0.0661 ± 0.0534
R	0.6528 ± 0.0378	0.1912 ± 0.0573
I	0.5170 ± 0.0312	0.0425 ± 0.0603
	$3f_1$	
U	1.1027 ± 0.0796	0.0431 ± 0.0722
B	1.0000 ± 0.0631	0.0000 ± 0.0660
V	0.7143 ± 0.0416	0.0173 ± 0.0616
R	0.6071 ± 0.0414	0.1302 ± 0.0696
I	0.4732 ± 0.0341	0.0993 ± 0.0744
	f_3	
U	0.7881 ± 0.1147	0.0442 ± 0.1435
B	1.0000 ± 0.1030	0.0000 ± 0.0998
V	0.7152 ± 0.0697	0.0861 ± 0.0942
R	0.6291 ± 0.0652	0.1954 ± 0.1027
I	0.5497 ± 0.0564	0.1006 ± 0.1027
	$4f_1$	
U	1.0965 ± 0.1560	-0.1532 ± 0.1425
B	1.0000 ± 0.1241	0.0000 ± 0.1298
V	0.6930 ± 0.0804	-0.0219 ± 0.1222
R	0.5439 ± 0.0778	-0.1618 ± 0.1451
I	0.4649 ± 0.0666	-0.1653 ± 0.1469

has the same structure as a static star of the same effective temperature and gravity, is probably a reasonable one if the frequency of pulsation is low. At any rate this assumption is required in order to make progress with the current state of the art. The quantity, f_T, the amplitude of local effective temperature variation relative to radial displacement, is an important parameter in mode identification. It turns out that the calculation of f_T is sensitive to the treatment of convection in δ Sct models (Balona & Evers 1999). One way of overcoming this difficulty is to leave f_T as a free parameter to be determined by the observations using a χ^2 minimization technique (Daszyńska-Daszkiewicz, Dziembowski & Pamyatnykh 2003). Application of this method to δ Sct stars indicates that the simple mixing-length theory for convection is inadequate, since the observed values of f_T are not in agreement with the calculated values.

In mode identification we therefore have the option of leaving f_T as a free parameter to be determined by the observations themselves or to use the somewhat inadequate models to constrain the solution. We decided to use the latter option because leaving f_T free increases the number of parameters by two. We took the view that the effect

of rotation, in any case, would limit the accuracy of the results so there is nothing to be gained by leaving f_T as a free parameter. The uncertainty in f_T means, however, that not much importance can be placed in the resulting phase differences from the models. The amplitude of f_T is more reliable and we can place more confidence in the calculated amplitude ratios.

Balona et al. (2012) estimated the effective temperature $T_{\mathrm{eff}} = 7300 \pm 150$ K and luminosity $\log L/\mathrm{L}_\odot = 1.7 \pm 0.1$, which places the star roughly in the middle of the instability strip and at the end of core hydrogen burning. There is a thin convection zone of H and He I near the surface which might modify the phase of the eigenfunction, but our current understanding of convection is insufficient to calculate this effect with any certainty. We may thus expect good agreement with the models for the relative amplitudes in various wavebands but less good agreement for the relative phases.

The calculation of amplitude ratios and phase differences was performed using the FAMIAS software package (Zima 2008). The photometric module of the software package compares the observed parameters with a pre-computed grid of non-adiabatic models for a range of stellar parameters. The program produces amplitude ratios and phase differences in a number of different passbands which include the Geneva, Johnson/Cousins and Strömgren systems. In our case, we used the results from the Johnson/Cousins system normalized to the B filter.

Since the amplitude ratios depend to some extent on the stellar parameters, it is important to calculate these values over a sufficiently wide range of models centred on the best estimate of the parameters which we take to be mass $M/\mathrm{M}_\odot = 2.10$, effective temperature $T_{\mathrm{eff}} = 7300$ K and $\log g = 3.5$. We calculated amplitude ratios and phase differences for models in the range $7200 < T_{\mathrm{eff}} < 7400$ K and $3.3 < \log g < 3.7$. These models were used because they produced the closest match to the observed frequencies f_1, f_2 and f_3. In FAMIAS, models for δ Sct stars computed by the ATON code (Ventura, D'Antona & Mazzitelli 2008) and MAD (Montalbán & Dupret 2007). The results given by FAMIAS for different values of l are compared with the observed values in Fig. 3.

6 DISCUSSION

At moderate rotation rates and for close frequencies, a strong coupling exists between modes with l differing by 2 and of the same azimuthal order, m. A consequence of mode coupling is that modes of higher degree should be considered in photometric mode identification. Modes with nominal degree $l > 2$ acquire substantial $l \leq 2$ components and therefore are more likely to reach detectable amplitudes. In these circumstances, mode identification using amplitude ratios or phase differences becomes both aspect- and m-dependent (Daszyńska-Daszkiewicz et al. 2002).

V2367 Cyg is a surprisingly rapid rotator. It can therefore be expected that problems involving mode coupling will be significant and that non-adiabatic quantities calculated from non-rotating models will not be very reliable. In particular, we expect that the observed amplitude ratios for f_2 will be intermediate between $l = 0$ and $l = 2$ if mode coupling is indeed present in this mode as suggested by Balona et al. (2012).

From Fig. 3, we see that f_1 could be $l = 0$, 1 or 3. Unfortunately in this range of stellar parameters there is no discrimination between these three spherical harmonic degrees in the amplitude ratio. The phase differences are intermediate between $l = 0$ and $l = 1$. What we can conclude is that our results for f_1 are certainly consistent with $l = 0$ and exclude $l = 2$.
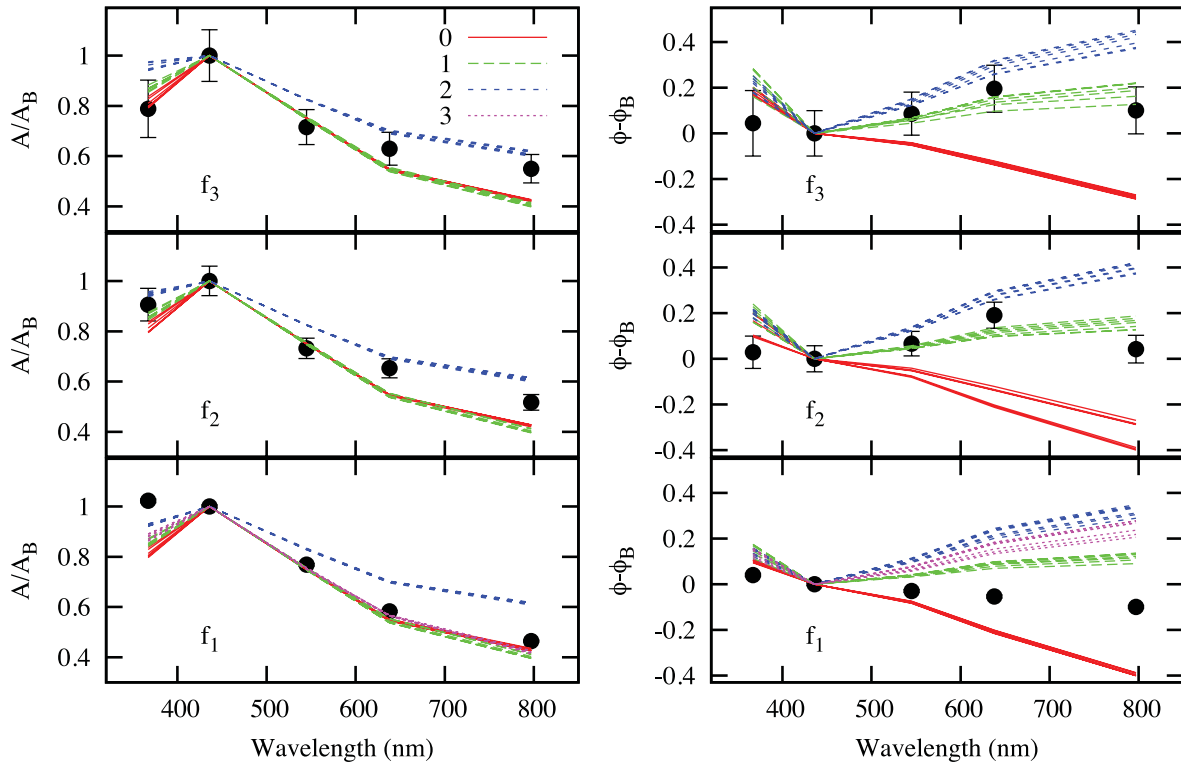
Figure 3. Amplitude ratios (left-hand panels) and phase differences (radians, right-hand panels) for f_1, f_2 and f_3. The curves are from models with a range of stellar parameters of the best estimated values with a range of stellar parameters of $7200 < T_{\text{eff}} < 7400$ K and $3.3 < \log g < 3.7$, and for different spherical harmonic degrees, $l(0 < l < 3)$.

Table 4. Zero points in the *UBVRI* filters for various sites and the number of observations, N.

Site	U	N		
Mexico	-0.078 ± 0.001	448		
USA	-0.033 ± 0.003	44		

Site	B	N	V	N
Bulgaria	-0.193 ± 0.003	220	-0.079 ± 0.002	221
Italy	-0.210 ± 0.002	372	-0.120 ± 0.002	412
Mexico	-0.170 ± 0.001	1319	-0.081 ± 0.001	2152
Turkey	-0.205 ± 0.001	1955	-0.121 ± 0.001	2128
USA	-0.170 ± 0.007	50	-0.066 ± 0.005	49

Site	R	N	I	N
Bulgaria	-0.007 ± 0.002	220	0.075 ± 0.002	220
Italy	-0.037 ± 0.001	410	0.056 ± 0.001	399
Mexico	0.091 ± 0.001	395	0.092 ± 0.001	375
Turkey	-0.057 ± 0.001	2052	-0.002 ± 0.001	2008
USA	0.013 ± 0.004	50	0.092 ± 0.004	46

For f_2 the amplitude ratios are intermediate between $l = 0$ and $l = 2$, as might be expected if this is a coupled mode. The phase differences are in agreement, though clearly no definite conclusion can be made on this basis alone. We conclude that mode coupling, as proposed by Balona et al. (2012), is consistent with our results. Results for f_3 are less reliable owing to the smaller amplitude, but are very similar to f_2, so this might again be a coupled mode.

Our overall conclusion from multicolour photometry is that mode identification is in agreement with the identifications proposed by Balona et al. (2012), but that the complexity introduced by the rapid rotation of V2367 Cyg produces severe limitations on any interpretation. We certainly cannot find any evidence to contradict the identifications, which in itself is a useful result.

Although HADS stars are of particular interest as they offer insights into non-linear phenomena, the class itself is very poorly defined. There is no particular reason why the pulsation amplitude should be used as a criterion. Perhaps a better definition of the class is the presence of harmonics of the dominant frequency or of
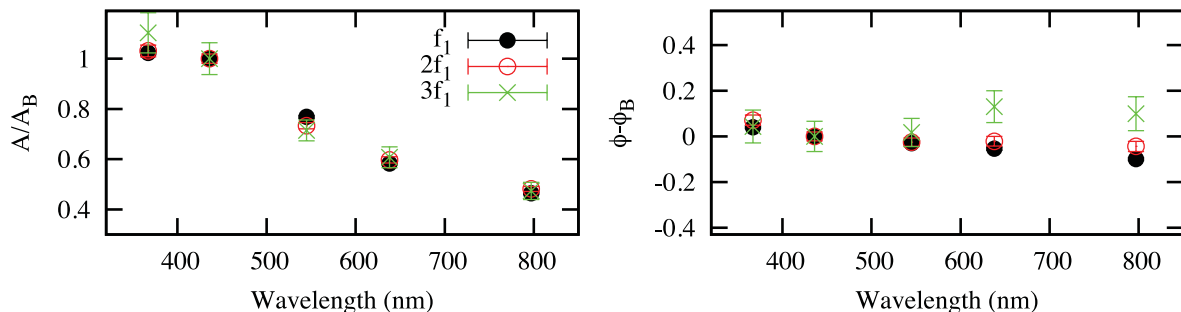

Figure 4. Amplitude ratios (left-hand panel) and phase differences (radians, right-hand panel) for f_1 and its harmonics, $2f_1$, $3f_1$.
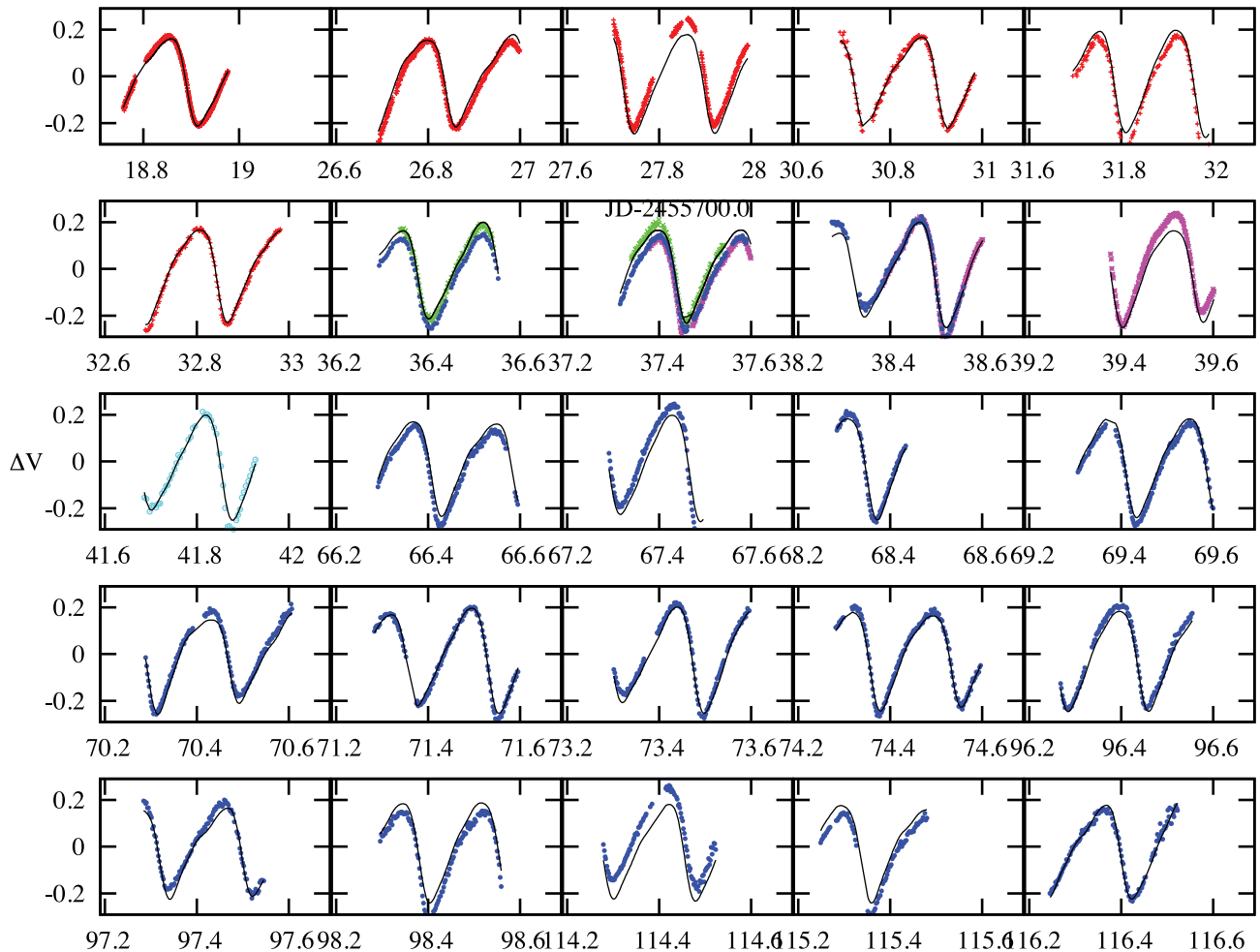
Figure 5. Light curves corrected for zero-points showing the fitted-Fourier curve.

combination frequencies. It would also be very important to refine the physical parameters of HADS. If they are indeed intermediate between δ Sct stars and Cepheids, they should line in a region of the HR diagram between these two classes of stars. More precise effective temperatures and luminosities are required to test this hypothesis.

REFERENCES

Akerlof C. et al., 2000, AJ, 119, 1901
Balona L. A., 2012, MNRAS, 422, 1092
Balona L. A., Evers E. A., 1999, MNRAS, 302, 349
Balona L. A. et al., 2012, MNRAS, 419, 3028
Breger M., 2007, Commun. Asteroseismol., 150, 25
Daszyńska-Daszkiewicz J., Dziembowski W. A., Pamyatnykh A. A., Goupil M., 2002, A&A, 392, 151
Daszyńska-Daszkiewicz J., Dziembowski W. A., Pamyatnykh A. A., 2003, A&A, 407, 999
Dziembowski W., 1977, Acta Astron., 27, 95
Hubeny I., Lanz T., Jeffery C. S., 1994, in Newsletter on Analysis of Astronomical Spectra, CCP7, Vol. 20, p. 30
Jin H., Kim S., Kwon S., Youn J., Lee C., Lee D., Kim K., 2003, A&A, 404, 621

Krtička J., 1998, in Dusek J., Zejda M. (eds), 29th Conference on Variable Star Research. Brno, Czech Republic, p. 73

Kupka F., Piskunov N., Ryabchikova T. A., Stempels H. C., Weiss W. W., 1999, A&AS, 138, 119

Kurucz R. L., 1993, SYNTHE Spectrum Synthesis Programs and Line Data. CD-ROM 18, Smithsonian Astrophysical Obs., Cambridge, Mass., USA

Lenz P., Pamyatnykh A. A., Breger M., Antoci V., 2008, A&A, 478, 855

Montalbán J., Dupret M.-A., 2007, A&A, 470, 991

Montgomery M. H., 2005, ApJ, 633, 1142

Mulet-Marquis C., Glatzel W., Baraffe I., Winisdoerffer C., 2007, A&A, 465, 937

Petersen J. O., 1973, A&A, 27, 89

Pigulski A., Pojmański G., Pilecki B., Szczygieł D. M., 2009, Acta Astron., 59, 33

Poretti E. et al., 2005, A&A, 440, 1097

Soszynski I. et al., 2008, Acta Astron., 58, 163

Stetson P. B., 1987, PASP, 99, 191

Suárez J. C., Garrido R., Goupil M. J., 2006, A&A, 447, 649

Suárez J. C., Garrido R., Moya A., 2007, A&A, 474, 961

Uytterhoeven K. et al., 2011, A&A, 534A, 125U

Ventura P., D'Antona F., Mazzitelli I., 2008, Ap&SS, 316, 93

Wu Y., 2001, MNRAS, 323, 248

Yeates C. M., Clemens J. C., Thompson S. E., Mullally F., 2005, ApJ, 635, 1239

Zima W., 2008, Commun. Asteroseismol., 157, 387